REMARKS

With the entry of the foregoing Amendments, Claims 18-23 and 42-45 are pending in this application. Claims 1-17 and 24-41 were previously cancelled without prejudice. Favorable consideration is requested.

At the outset, applicant requests the withdrawal of the "finality" of the Office Action because all of the following identified objections and rejections were never raised before -- even though they could have been raised in a prior Office Action because all of these objections and rejections target parts of the specification and claims that were in existence prior to the Amendment filed on December 29, 2008. Thus, applicant has never had a chance to address all of these new objections and rejections. In summary, the following objections and rejections were never raised before and should have been raised in a non-final Office Action:

1. The Examiner's objections in paragraph number 2 of the Detailed Action.
2. The Examiner's objections in paragraph number 3 of the Detailed Action.
3. The Examiner's objections in paragraph number 4 of the Detailed Action.
4. The Examiner's rejections in paragraph numbers 6-7 of the Detailed Action.
5. The Examiner's objection in paragraph number 8 of the Detailed Action.
6. The Examiner's contentions in paragraph number 9 of the Detailed Action.
7. The Examiner's contentions in paragraph number 10 of the Detailed Action.
8. The Examiner's contentions in paragraph number 11 of the Detailed Action.
9. The Examiner's rejections in paragraphs 12-13 of the Detailed Action.

All of the foregoing objections and rejections were never raised in a non-final Office Action. Thus, the "finality" of the subject Office Action is improper. Applicant respectfully requests the withdrawal of the "finality" of the Office Action.

Turning to the amendments of the specification, and the amendments of the claims, the amendments are in line with the helpful suggestions of the Examiner as set forth in the Office Action and discussed below, and the new claims are combination of some of the original claims. No new matter has been added by the amendments, which are fully supported by the specification, as discussed below.

In paragraph no. 2 of the Detailed Action, the Examiner has objected to the repetitive paragraphs beginning on lines 4 and 15 of page 8 of the specification. The Examiner is correct. In response, the specification has been amended.

In paragraph no. 3 of the Detailed Action, the Examiner has contended that the Figures do not show the spin valve and its details. Applicant disagrees. Figures 3, 4A and 4B show the spin valve and its corresponding layers, including the spacer layer 113 and 133 in the Figures.

In paragraph no. 4 of the Detailed Action, the Examiner has objected to the drawings because they use reference no. 123 (Figure 5). Applicant has addressed this issue by changing reference no. 113 in lines 24 and 29 on page 9 of the specification to reference no. 123.

In paragraph nos. 6-7 of the Detailed Action, the Examiner has rejected claims 18-23 as allegedly being indefinite for the specific reasons identified in paragraph nos. 8-11, as discussed below.

In paragraph 8, the Examiner is correct that the claim 18 phrase "spacer element" should be amended to "spacer layer." Applicant has amended the claim in this fashion.

In paragraph 9, there is a question about the use of the word "substrate" in the context of the "spacer layer." In response, applicant notes that the spacer layer is formed using a substrate 31 as shown in Figures 2A-2C (and note that Figure 2C = Figure 6) and as described in the corresponding parts of the specification beginning on page 4, line 6. The substrate structure 31

in Figure 2C is the spacer layer 113 shown in Figures 4A and 4B and is also the spacer layer 133 shown in Figure 6 (all of which is supported by original claim 18). In addition, as noted on page 6, lines 25-26, the substrate 31 can be laid onto any other substrate. Moreover, the specification clearly teaches that the spin valve comprises these stacked layers. See, for example, Figure 3 and page 7, lines 5-7, and Figure 6 and page 10, line 30 to page 11, line 14.

In paragraph 10, with reference to Figure 5, the Examiner contends that the specification does not provide support for a spacer layer where the mesoscopic portion of the spacer layer is a semiconductor. In response, we direct the Examiner's attention to Figure 5 and page 9, line 15 to page 10, line 21 (and with the amendment of "113" to "123" in lines 24 and 29 on page 9 of the specification; amendment of "113" to "123" in line 1 on page 10 of the specification; and amendment of "113" to "123 or 133" in line 16 on page 10 of the specification). Thus, the specification does provide support.

In paragraph 11, the Examiner rejects claim 20 by contending that the spacer layer comprising a matrix (which is dielectric) is in conflict with the claimed use of a semiconductor substrate 31 to form the spacer layer. In response, we traverse this rejection by directing the Examiner's attention to page 10, lines 5-34 as well as the descriptions above concerning paragraph 9 of the Detailed Action.

In paragraphs 12-13, the Examiner rejects dependent claims 19-23 on the grounds that they stem from independent claim 18 for the reasons stated above. In response, this rejection of claims 19-23 is moot in view of the positions set forth above for claim 18.

In paragraphs 14-22, the Examiner rejects claims 18-23 as allegedly anticipated (lacking novelty) by Fujiwara (US Published Patent Application Number 2002/0054461). In response,

we traverse this rejection because Fujiwara does not disclose each and every feature in independent claim 18.

Fujiwara makes reference to obtaining a mosaic structure like the one depicted in Figure 3b. However, this figure is simply a schematical representation of a sequence of conductive and insulating parts having a pillar structure. Significantly, the corresponding written description states:

> "[0022] The thin non-magnetic layer structure or conducting layer part 33 includes essentially two parts with significantly different conductivities, typically a conductor part 33a having low resistivity and an insulator part 33b having high resistivity, as depicted schematically in FIG. 3b. This kind of **mosaic structure** can be made using various methods. One of the preferable methods is a co-deposition of conducting material(s) and insulating material(s) that are essentially immiscible to each other. The conducting materials are preferably selected from the group of Ag, Al, Au, Cr and Cu and their alloys and the insulating materials are preferably selected from the group of the oxides of any elements such as Al, Cr, Cu, Mg, Mn, Nb, Pd, Si, Ta, Ti, V and Zr or the group of nitrides of any elements such as Al, B, C, Si and Ta. This method can be substituted by an alternate method that after making a layered structure of both conducting material(s) and insulating material(s) the layered structure is heat-treated resulting in a **mosaic structure**. Another is that after a co-deposition of immiscible metals, one of which is easier to oxidize than the other, the deposited layer is exposed to an oxidizing atmosphere. Instead of oxidation, nitrogenation may work if materials with different easiness in nitrogenation are chosen. [0023] The **mosaic**

structure described above can include any inhomogeneous lateral distribution of at least two kinds of parts with a resistivity substantially different from each other, such as a structure with metallic pillars embedded in an insulator medium and a structure with a metal defused into the grain-boundaries of insulator grains." (emphasis added)

On the basis of the above excerpt of the Fujiwara description is apparent that:

i. Fujiwara deals in a very generic way with a mosaic structure which can be any "lateral distribution" of two kinds of parts with different resistivity, providing, as examples, "metallic pillars embedded in an insulator" and "metal defused in grain boundaries of insulator grains;"

ii. Fujiwara mentions two co-deposition methods and a layered deposition method;

Based on the above, it can be concluded in the first place that Fujiwara thus merely outlines a framework in which metallic and insulant parts are mixed, but does not give any hint regarding the microstructure of the composite, i.e., its crystalline structure that deeply influences the electrical and magnetical behavior of the material. As a result, there is no anticipation.

Furthermore, the methods mentioned by Fujiwara do not lead to the production of a material with properties similar to that of the claimed material.

It must first be noted that while in the subject application it is presently claimed that "a semiconductor or dielectric substrate (31) is subjected to a chemical etching process to form pores (22; 134) in said semiconductor or dielectric substrate (31)," i.e., the device includes a

substrate with pores, the Fujiwara reference does not mention any pore or porous structure. The spacer layer obtained by the claimed process, at the end of the process, is still a nanoporous substrate retaining is pores, although filled with metal, and the corresponding distribution of pores. There is no indication in Fujiwara to obtain a similar structure. As a result, there is no anticipation.

From the Fujiwara reference, it is not possible to ascertain which filler/matrix nanowire based composite structure can be grown, in particular which structural properties (in terms of amorphous/microcrystalline/monocrystalline phase and relative orientation) the layer 33 of Fujiwara will have, and even less can be said, on the basis of what is disclosed by Fujiwara on the resulting electrical or magnetical properties.

However, it is widely acknowledged that by co-deposition the resulting material properties are the "effective" superposition of the filler and matrix original properties. By co-deposition, the filler and the matrix material, even if are mixed up at proper rates will always bring into the final composite material their original crystal structure. It is known to every expert in the field that the properties of similar "mosaic structures" depend heavily on the structure of the phases (e.g., monocrystalline, micro-crystalline, nano-crystalline, amorphous) composing the mosaic.

There is then a further very important feature, which is closely tied to having a nanoporous substrate. Nanowires grown in the pore of porous template, for instance, by electrodeposition, are different from nanowires grown by other methods, i.e., Fujiwara codeposition. The (nanometric) geometrical constraints imposed by the nanopores determine specific types of growth of the wires, according to deposition conditions, allowing control of the crystalline growth through the control of the deposition parameters (electrodeposition in

particular). In this regard, attached is a publication, i.e., M. Darques, L. Piraux, A. Encinas, P. Bayle-Guillemaud, A. Popa and U. Ebels, Appl. Phys. Lett. **86**, 0725008, (2005), which depicts the way electrodeposition in the nanopores can be controlled for tailoring the crystal structure of the filling material by the process parameters, e.g., the pH of the electrolyte, in order to obtain anisotropy. It is largely acknowledged that the properties of anisotropy of materials, which are of utmost importance in determining the properties of the spacer layer, are tightly linked to their crystal structure. In other words, a nanoporous material with nanowires grown in the nanopores has a complex of electrical properties and, most important, magnetical properties that cannot be replicated by the composite described by Fujiwara. Thus, for these additional reasons, there is no anticipation.

In view of the foregoing information, applicant requests the withdrawal of the anticipation rejection because the cited reference does not disclose each and every feature in the claims.

For at least the reasons stated above, applicant submits that this application is in condition for allowance. A notice to that effect is earnestly solicited.

Respectfully submitted,

NIXON & VANDERHYE P.C. Reg No 32,933

By: Meryl J. Wilson
(for) Duane M. Byers
Reg. No. 33,363

DMB:lfo
901 North Glebe Road, 11th Floor
Arlington, VA 22203-1808
Telephone: (703) 816-4000
Facsimile: (703) 816-4100

HTML ABSTRACT + LINKS

APPLIED PHYSICS LETTERS 86, 072508 (2005)

Electrochemical control and selection of the structural and magnetic properties of cobalt nanowires

M. Darques[a] and L. Piraux
Unité PCPM, Université Catholique de Louvain, Place Croix du Sud 1, B-1348, Louvain-la-Neuve, Belgium

A. Encinas
Instituto de Física, Universidad Autónoma de San Luis Potosí, Av. Manuel Nava 6, Zona Universitaria, 78290 San Luis Potosí, S.L.P., Mexico

P. Bayle-Guillemaud, A. Popa, and U. Ebels
CEA-DRFMC, 17 rue des Martyrs, 38054 Grenoble, Cedex 9, France

(Received 21 June 2004; accepted 13 January 2005; published online 10 February 2005)

In this letter we present a convenient way of controlling the direction of the uniaxial magnetocrystalline anisotropy in arrays of electrodeposited hcp Co nanowires. Combining electron microscopy and ferromagnetic resonance measurements, it is shown that using an appropriate *p*H of the electrolytic solution, the hcp *c* axis can be oriented parallel or perpendicular to the wires axes simply by changing the deposition current density or deposition rate. This reorientation of the *c* axis leads to a drastic change in overall magnetic anisotropy as the crystal anisotropy either competes for perpendicular oriented *c* axis or adds to the shape anisotropy for parallel oriented *c* axis. © *2005 American Institute of Physics*. [DOI: 10.1063/1.1866636]

Among the different magnetic nanowires produced until now, cobalt has been the focus of much attention motivated by its large crystal anisotropy when growth occurs in the hcp structure. Indeed, numerous reports have shown that electrodeposition of Co nanowires leads to a "polycrystalline" structure in which hexagonal close packing (hcp) is the usual structure for most grains. Under usual deposition conditions, these grains exhibit preferred orientation of the hexagonal axis within a few degrees normal to the wire axis and are randomly distributed.[1,2] In this case, the large magnetocrystalline anisotropy competes directly with shape anisotropy which tends to align the magnetization along the wire axis, giving rise to a lowering of the effective anisotropy. Furthermore, the coexistence of varying amounts of the two hcp and fcc cobalt phases was found by several groups.[3–5] These observations constitute a major drawback in the use of Co nanowire arrays in applications such as perpendicular recording media, where an alignment of the *c* axis along the wire axis is desired. This underlines the importance of controlling the microstructure and in particular the magnetic easy axis of the electrodeposited nanowires.

Though a thorough understanding of the mechanism participating in the formation of Co films by electrodeposition is still lacking, the phase selection as related to deposition conditions or substrate influence has been studied in detail.[6–8] From these studies, the electrolytic bath acidity, or *p*H, is known to be the most important parameter in determining the structure of electrodeposited cobalt. Other relevant parameters of the operative conditions in cobalt electrocrystallization, though minor ones compared to the *p*H, are the current density and temperature of deposition.[9]

In a previous study our group has shown the role of the *p*H for the control of the orientation of the hcp *c* axis in arrays of Co nanowires. In particular a reorientation of the hcp *c* axis along the wires axes could be obtained for *p*H above 6.0.[10] In contrast to this previous study, we show here that besides the *p*H, the deposition rate, or current density, strongly affects the growth process of the cobalt nanowires. In particular, it leads to a significant shift of the critical *p*H range where the reorientation of the *c* axis from a perpendicular to a longitudinal direction occurs. As a consequence, for a limited *p*H range (5–6), it is possible to selectively obtain high quality Co nanowires with either a parallel or a perpendicular orientation of the *c* axis only by changing the deposition current. This makes it possible to control in a very simple way the overall magnetic anisotropy.

Arrays of Co nanowires are grown by electrodeposition into the cylindrical pores of lab-made track-etched polycarbonate membranes using a standard three-probe technique. The diameter of the pores is 30 nm with membrane porosity, *P*, of 3.5% (5×10^9 pores per cm^2). Prior to deposition a Cr (20 nm)/Au (300 nm) layer is evaporated on one face of the membrane to serve as a cathode. The electrolyte is 250 g/l $CoSO_4$, $7H_2O$ and 30 g/l H_3BO_3, the *p*H of the as-prepared solution is 4.0 and adjusted with diluted NaOH. Galvanostatic room temperature deposition is done with current densities set from 5 to 50 mA/cm^2, over a constant membrane surface of 1.2 cm^2. Structural characterization has been done by transmission electron microscopy (TEM) after dissolving the polycarbonate membrane and spreading of the wires onto a grid.

As shown in a previous report,[10] the average, or dominant orientation, of the *c* axis induces significant changes in the total effective anisotropy of the system. Therefore, the effects of the deposition current on the electrocrystallization characteristics have been determined by measuring the uniaxial crystal anisotropy field H_U in arrays of nanowires as a function of both the deposition current and the *p*H of the electrolyte. For this purpose, ferromagnetic resonance (FMR) measurements were carried out using a microstrip transmission line.[10]

[a]Author to whom correspondence should be addressed; electronic mail: darques@pcpm.ucl.ac.be

 © 2005 American Institute of Physics
Downloaded 11 Feb 2005 to 130.104.231.145. Redistribution subject to AIP license or copyright, see http://apl.aip.org/apl/copyright.jsp

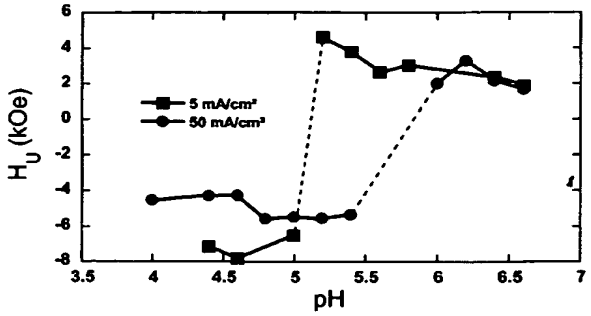

FIG. 1. The value of magnetocrystalline anisotropy field as a function of the pH for 30 nm Co nanowires electrodeposited at current densities of 5 and 50 mA/cm^2.

At a given constant frequency f, the ferromagnetic resonance conditions when the magnetic field is swept parallel to the wires are:
(i) c axis and, hence, magnetocrystalline easy axis parallel to the wire axis ($H_U>0$):

$$\frac{f}{\gamma}=H_R+2\pi M_S(1-3P)+H_U, \tag{1}$$

(ii) c axis and, hence, magnetocrystalline easy axis perpendicular to the wire axis ($H_U<0$):

$$\left(\frac{f}{\gamma}\right)^2=[H_R+2\pi M_S(1-3P)+H_U]\times[H_R+2\pi M_S(1-3P)]. \tag{2}$$

In Eqs. (1) and (2), γ(Co)=3.05 GHz/kOe, H_R is the resonance field, $2\pi M_S\sim 8.8$ kOe is the shape anisotropy field [M_S(Co)$\sim$1370 emu/cm^3] and $6\pi M_S P$ is the dipolar coupling field between the wires ($\sim$900 Oe for P=3.5%).[10] Therefore, FMR studies provide a direct quantification of the anisotropy crystal field.

Measurements were performed at room temperature by sweeping down the magnetic field applied parallel to the wires from 10 kOe to zero, at different constant excitation frequencies up to 50 GHz, see Ref. 10 for further details. The crystal anisotropy field is obtained by fitting expressions (1) and (2) once the resonance field has been determined at different frequencies.[11]

Figure 1 shows the variation of the crystal anisotropy field as a function of the pH for samples deposited using a high current density of 50 mA cm^{-2} (circles) and a low current density of 5 mA cm^{-2} (squares).

For both deposition currents, the overall dependence of the crystal anisotropy field is similar. In particular, H_U is negative at low pH and positive at high pH, which is consistent with a dominant fraction of grains having (a) the c axis perpendicular ($H_U<0$) and, (b) the c axis parallel ($H_U>0$) to the wires axes. However, the change in sign for H_U takes place around different pH values depending on the deposition current density. At higher deposition currents, the crystal anisotropy fields are in the range of -4.0 to -5.5 kOe for pH values between 4.0 and 5.5. Above this pH value, H_U rapidly increases and reaches values around +2 to +3 kOe for a pH above 6.0. For low deposition currents, the increase in H_U, takes place at considerable lower pH values, around 5.0, and the transition is also more abrupt

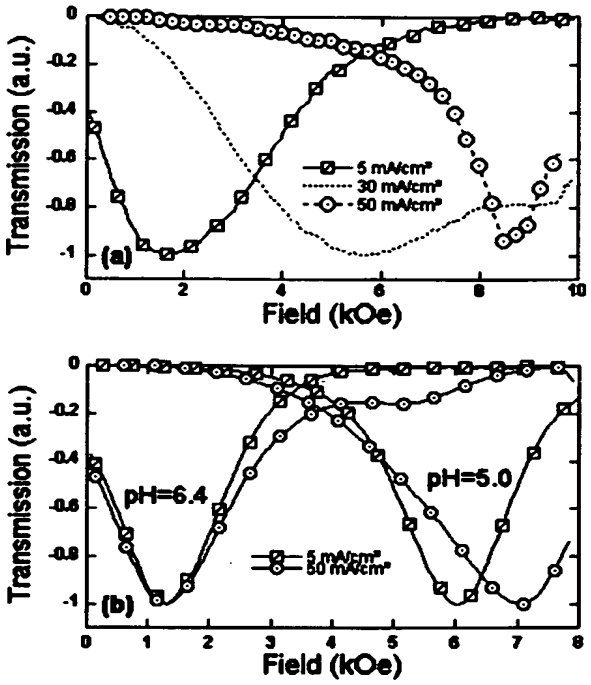

FIG. 2. FMR spectra with a magnetic field applied parallel to the wires for 30 nm Co nanowires grown (a) at pH 5.2 and current densities of 5, 30, and 50 mA/cm^2 recorded at 43 GHz and, (b) at pH 5.0 and 6.4 with current densities of 5 and 50 mA/cm^2 recorded at 35 GHz.

than at high currents. At pH 5.2, H_U reaches a maximum value of +4.6 kOe, and then decreases slowly as the pH increases until it reaches a value of 2 kOe at a pH of 6.6.

As suggested by these results (Fig. 1), the effect of the current is to shift the pH value at which the structural and magnetic changes take place. Specifically, the lowering of the deposition current shifts this transition to lower pH values.

Another remarkable and important property derived from Fig. 1 is that, in a limited pH range, both structural phases (c axis parallel and perpendicular to the wires) can be obtained from the same electrolyte simply by changing the deposition current. This is illustrated in Fig. 2(a) which shows the resonance spectra measured in two Co nanowire arrays deposited from a pH 5.2 electrolyte using high and low currents (indicated in the figure). As can be observed, by changing the current density from 50 down to 5 mA cm^{-2}, the resonance field can change as much as 8 kOe, which is consistent with a dominant fraction of hcp Co grains having their c axis perpendicular (high current) and parallel (low current) to the wires axes. Figure 2(a) also shows an absorption curve measured on a sample grown at an intermediate deposition current (30 mA cm^{-2}). In this case, a much broader peak appears as a clear signature of the inhomogeneous crystallographic structure of the so-prepared Co nanowires. In these same lines, and in agreement with the results in Fig. 1, below and above a pH of 5.0 and 6.0, respectively, the orientation of the c axis is independent of the deposition current. This is shown in Fig. 2(b) for high pH (6.4), and low pH (5.0). To be noted is that for the pH 5.0 samples, the resonance fields for the two deposition currents

Downloaded 11 Feb 2005 to 130.104.231.145. Redistribution subject to AIP license or copyright, see http://apl.aip.org/apl/copyright.jsp

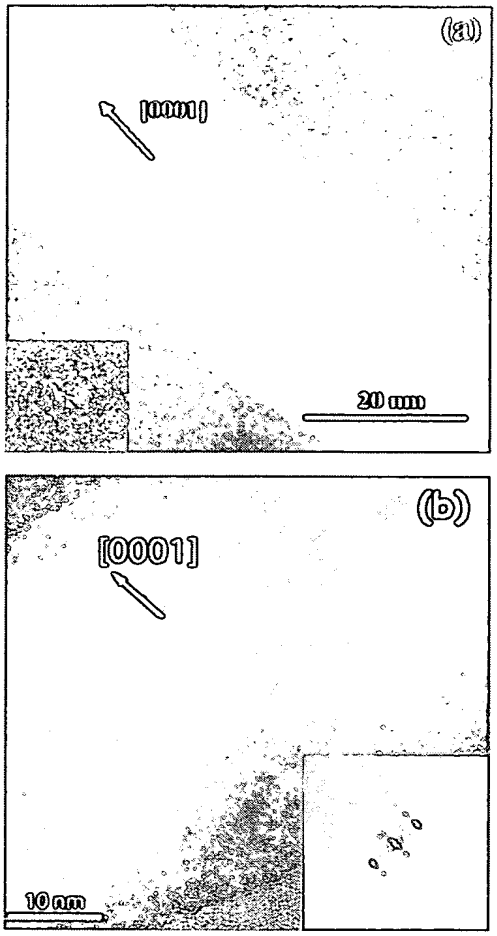

FIG. 3. TEM bright field images and corresponding diffraction patterns of two 30 nm Co nanowires electrodeposited at pH=5.2 and current densities of (a) 5 and (b) 50 mA/cm^2.

differ, but these values are consistent with a c axis oriented perpendicular to the wire axis.

The dependence of the hcp c-axis orientation on the deposition current is corroborated by TEM investigations as shown in Figs. 3(a) and 3(b) for Co wires deposited at a pH of 5.2. In the case of low current density [Fig. 3(a)], the TEM bright field and diffraction images clearly show an orientation of the c axis oriented parallel to the wire axis (+/−5°). Similarly, in the case of high current density [Fig. 3(b)], the TEM bright field and diffraction images clearly show an orientation of the c axis oriented perpendicular to the wire axis (+/−5°). Although only short sections are shown in the images, no grain boundaries were observed along longer sections of the ten wires that have been examined in detail.

As pointed out in previous works involving electroplated Co films, these structural changes can be attributed to the influence of absorbed hydrolysis products at the cathode as well as to evolution of hydrogen, which are known to depend on the pH and the plating current.[9,12] For bulk hcp Co, the magnetocrystalline anisotropy has an upper bound of 7.8 kOe[13] ($K=5.3\times10^6$ erg/cm^3 and $H_U=2K/M_S$). It is noted that for perpendicularly oriented c axis, the maximum crystal anisotropy field found in this study (~7.8 kOe) corresponds closely to the earlier mentioned upper bound. Such large values are consistent with the very good structural quality demonstrated by our TEM studies. In contrast, values for H_U are well below the maximum expected value when the c axis is parallel to the wires. Furthermore, a gradual decrease of H_U with increasing pH clearly appears. This behavior can be associated to the influence on crystalline growth by adsorbed hydrolysis products (such as Co hydroxides) at the cathode when the pH is sufficiently high. Another possible reason for the reduction of H_U are stacking faults, which might increase in number in the high pH samples.[14] However, further structural characterization is required to provide a better understanding on the relation between the growth, crystalline structure and the value of the magnetocrystalline anisotropy field.

In conclusion, the crucial role of the deposition current on the preferential orientation of the hcp c axis in Co nanowires with respect to the wire axis has been shown. In particular, both structural phases, hcp Co with the c axis parallel and the c axis perpendicular to the wires, can be obtained from a single electrolyte by changing the deposition current in a limited pH range (5.0–5.5) by one order of magnitude. This reorientation of the c axis leads to changes in sign of the crystalline anisotropy field. This allows not only to chose the desired orientation of the c axis, but also to simply grow wires in which both phases are alternated, providing a simple and convenient way to control the magnetic properties of electrodeposited cobalt nanowire arrays to a large extent.

The authors would like to thank R. Legras and E. Ferain for providing the polycarbonate membrane samples used in this study, Th. Fournier for fabrication of Si/SiN membranes used in the TEM experiments, and Dr. L. Vila for his valuable help in the experiment. This work was supported in part by the European Program Contract No.: HPRN CT1999 00150 as well as by the Belgian Science Policy through the Interuniversity Attraction Pole Program PAI (5/1/1). One of the authors (A.E.) thanks CONACyT for financial support through Grant No. J-40426.

[1] J. L. Maurice, D. Imhoff, P. Etienne, O. Durand, S. Dubois, L. Piraux, J.-M. George, P. Galtier, and A. Fert, J. Magn. Magn. Mater. **184**, 1 (1998).
[2] R. M. Metzger, V. V. Konovalov, M. Sun, T. Xu, G. Zangari, B. Xu, M. Benakli, and W. D. Doyle, IEEE Trans. Magn. **36**, 30 (2000).
[3] V. Scarani, B. Doudin, and J.-P. Ansermet, J. Magn. Magn. Mater. **205**, 241 (1999).
[4] G. J. Strijkers, J. H. J. Dalderop, M. A. A. Broeksteed, H. J. M. Swagten, and W. J. M. de Jonge, J. Appl. Phys. **86**, 5141 (1999).
[5] M. Kröll, W. J. Blau, D. Grandjean, R. E. Benfield, F. Luis, P. M. Paulus, and L. J. de Jongh, J. Magn. Magn. Mater. **249**, 241 (2002).
[6] S. Nakahara and S. Mahajan, J. Electrochem. Soc. **127**, 283 (1980).
[7] T. A. Tochitskii, A. V. Boltushkin, and V. G. Shadrov, Russ. J. Electrochem. **31**, 178 (1995).
[8] I. M. Croll, IEEE Trans. Magn. **23**, 59 (1987).
[9] T. Chen and P. Cavallotti, Appl. Phys. Lett. **41**, 205 (1982).
[10] M. Darques, A. Encinas, L. Vila, and L. Piraux, J. Phys. D **37**, 1411 (2004).
[11] In a first fit, H_u was obtained using Eq. (1). When H_u turned out to be negative, the fit was repeated using Eq. (2).
[12] T. Cohen-Hyams, W. D. Kaplan, and J. Yahalom, Electrochem. Solid-State Lett. **5**, C75 (2002).
[13] E. Du Tremolet de Lacheisserie, in *Magnétisme*, edited by J. Bornarel (Presses Universitaires de Grenoble, Grenoble, 1999), p. 168.
[14] B. Bian, W. Yang, D. Laughlin, and D. Lambeth, IEEE Trans. Magn. **37**, 1456 (2001).

Downloaded 11 Feb 2005 to 130.104.231.145. Redistribution subject to AIP license or copyright, see http://apl.aip.org/apl/copyright.jsp